

000 001 002 003 004 005 006 007 008 009 010 011 012 013 014 015 016 017 018 019 020 021 022 023 024 025 026 027 028 029 030 031 032 033 034 035 036 037 038 039 040 041 042 043 044 045 046 047 048 049 050 051 052 053 TWINSHIELD: SECURE FOUNDATION MODEL EXECUTION BY UNIFYING TEES AND CRYPTO-PROTECTED ACCELERATORS

006
007
008
009
010
011
012
013
014
015
016
017
018
019
020
021
022
023
024
025
026
027
028
029
030
031
032
033
034
035
036
037
038
039
040
041
042
043
044
045
046
047
048
049
050
051
052
053
Anonymous authors

Paper under double-blind review

ABSTRACT

Recent advances in Transformer-based foundation models (FMs) have driven significant developments across diverse AI tasks, facilitating their deployment in security-sensitive domains. Despite their capabilities, FMs impose substantial inference costs, driving reliance on third-party cloud infrastructure equipped with high-performance computation resources. However, these cloud platforms cannot be fully trusted and remain vulnerable to data breaches, introducing dual confidentiality challenges: protecting user data from exposure and safeguarding models against unauthorized access. Mainstream protection mechanisms leverage trusted execution environments (TEEs), where confidentiality and integrity are enforced through hardware-based isolation, encryption, and integrity verification. But executing inference entirely within TEEs incurs a significant overhead, which is further exacerbated in large-scale FMs. Recent studies have proposed schemes that combine TEEs with untrusted accelerators (e.g., GPUs) to offload partial inference operations. However, prior offloading schemes cannot solve dual confidentiality challenges in FM inference, since operations such as Attention depend on dynamic operands that prevent secure precomputation and must remain within TEEs. Moreover, the communication overhead between TEEs and accelerators grows dramatically with model scale, constituting a new system design challenge for FMs. To address these challenges, we propose TwinShield, a framework that enables secure inference of Transformer-based FMs in heterogeneous TEE–accelerator systems with dual protection for both model and data. TwinShield improves efficiency through *protocol-level* outsourcing, which securely offloads the majority of operations to accelerators, and enhances throughput via a *system-level* design that overlaps TEE preparation, communication, and accelerator execution. Our evaluation on representative LLMs and VLMs shows that TwinShield offloads about 87% of computations to accelerators and achieves $3.3 \times$ – $5.1 \times$ speedups over baselines. The code is publicly available at <https://anonymous.4open.science/r/Twinshield>.

1 INTRODUCTION

With the rapid advances in Transformer architectures (Vaswani et al., 2017), they have been widely applied in domains such as computer vision (Dosovitskiy et al., 2020) and natural language processing (Devlin et al., 2018). Building on this architecture, large-scale foundation models (FMs) such as LLaMA and Qwen have emerged. Benefiting from their remarkable capabilities, FMs are becoming increasingly popular and are being deployed in many critical scenarios. However, these capabilities are primarily driven by the enormous parameter sizes of such models, which consequently impose significant computational demands. To address the challenges of model size and deployment complexity, cloud-based Foundation Model-as-a-Service (FMaaS)¹ has become a widely adopted paradigm, enabling model owner to provide state-of-the-art FMs as inference services to end users in a cost-effective manner.

¹<https://builder.aws.com/building-a-foundation-model-as-a-service-fmaas-on-aws>

In the FMaaS, input data provided by clients, such as personal health information (e.g., sleep patterns, pulse, heart rate) and financial records, is highly sensitive. Meanwhile, model providers delegate the hosting and execution of their FMs to the cloud, which constitutes valuable intellectual property, since developing them requires enormous investments in data collection, domain expertise, and computational resources for training. Despite leveraging the cloud’s powerful computation resources, remote execution cannot be fully trusted, as adversaries may exploit privileged system software (Pahima, 2022) or hardware vulnerabilities (Tung, 2021) to compromise privacy and computation integrity. Therefore, guaranteeing the *confidentiality* of both client inputs and provider models, as well as the *integrity* of inference, is imperative for FMaaS.

Trusted Execution Environments (TEEs), such as Intel SGX, provide a trusted environment to safeguard the privacy and integrity of sensitive computations. In systems with TEEs, the CPU is treated as the root of trust. The processor shields individual secure enclaves from privileged system software attacks via hardware-enforced isolation. Furthermore, counter-mode encryption and integrity tree-based data verification are performed by the TEE hardware to protect against breaches and tampering with enclave off-chip data. Accordingly, prior studies have investigated the use of TEEs for secure machine learning inference. For instance, Hanzlik et al. (2021) proposed to store ML models in the secure enclave and perform inference completely in TEEs, hence protecting computation integrity and the confidentiality of all data. Unfortunately, deployment of the entire model inside TEEs introduces extremely high overhead due to the limited resources of TEEs. Recent advances in TEE-based accelerators (e.g., NVIDIA H100 confidential mode) attempt to mitigate this issue, but they remain vendor-specific, technically restrictive, and provide weaker guarantees than CPU-based TEEs. Subsequent works (Tramer & Boneh, 2018; Hashemi et al., 2021; Sun et al., 2023; Shen et al., 2022) attempt to improve the performance of TEE-based model inference by *outsourcing* heavy computations from TEEs to an untrusted external accelerator (e.g., GPUs, FPGAs and ASICs), and *verifying* the computation integrity inside the enclave. While the aforementioned secure outsourcing techniques enhance the system efficiency of TEE-only methods, they struggle to outsource sufficient computations of Transformer-based FMs to untrusted accelerators from trusted TEEs. The challenges are summarized as follows:

(I) *Confidential Attention Computation*: Traditional schemes for non-Transformer models rely on additive secret sharing to outsource linear operations $W \cdot x$ by sending the masked input $x + r$ to untrusted accelerator for $W \cdot (x + r)$ and recovering the result by subtracting the precomputable $W \cdot r$. In contrast, Attention involves computations such as $q \cdot k$ and $\text{softmax}(qk) \cdot v$, where both operands are generated at runtime. This property precludes precomputation and renders existing methods inapplicable. Moreover, prior studies in cloud settings (Tramer & Boneh, 2018; Hashemi et al., 2021) focus solely on input protection while assuming the model resides with the server, leaving it unprotected. Conversely, on-device approaches (Shen et al., 2022; Sun et al., 2023) focus on model privacy but treat user inputs as local and leave them unprotected. We argue that both the model and inputs must be protected simultaneously, a setting substantially more complex than safeguarding either alone. Achieving this dual protection requires obfuscating both components before outsourcing any operation to untrusted accelerators, necessitating a redesign of secure computation algorithms.

(II) *Significant Communication*: Foundation models contain billions of parameters, making accelerator-TEE communication non-negligible and increasingly costly. For example, outsourcing a single layer of LLaMA-8B can incur 3.38 GB of bidirectional data transfer. While prior works designed for small models such as CNNs tolerate this overhead, they become inefficient when applied to FMs. This scalability gap underscores the need for new system designs that mitigate the substantial communication inherent in outsourcing large-scale FMs.

To address these challenges, we propose TwinShield (as shown in Figure 1), a framework for confidential and verifiable inference on Transformer-based FMs. The model developer deploys the model on the cloud to process the client input. TwinShield’s protocol enables most computations

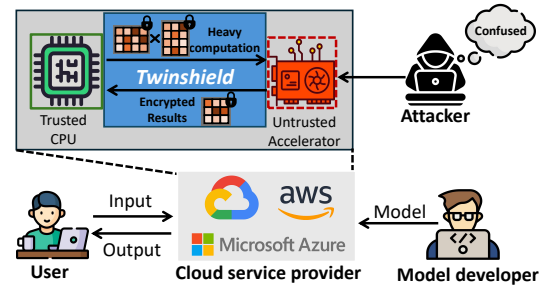


Figure 1: Overview of our trusted foundation models (FMs) inference, TwinShield.

108 to run on accelerators while ensuring data confidentiality and computation integrity. For Challenge
 109 (I), we design a confidentiality-guaranteed outsourcing protocol, OutMult, which consists of two
 110 components: OutAttnMult for Attention computations and OutLinearMult for weight–input
 111 multiplications, both ensuring protection of model and input. For Challenge (II), our key insight
 112 is that attention heads can be computed independently, which allows their workloads to be decom-
 113 posed into smaller parallel tasks. By pipelining TEE computation, data transfers, and accelerator
 114 computation across different heads, we effectively utilize the idle time. The proposed design, i.e.,
 115 OutPipe, overlaps communication and computation, thereby improving hardware utilization and
 116 increasing throughput by 52.4%. Through extensive experiments on various FMs, such as large
 117 language models (LLMs) and vision language models (VLMs), we show that TwinShield achieves
 118 substantial throughput improvements ranging from $3.3\times$ to $5.1\times$ for private verifiable inferences,
 119 without sacrificing accuracy.
 120

2 THREAT MODEL

123 We consider a cloud-based Foundation Model-as-a-Service (FMaaS) scenario with three parties: the
 124 model developer, the cloud service provider, and the model user, as illustrated in Figure 1. The model
 125 developer trains and then deploys a foundation model $f : X \rightarrow Y$ on the cloud service provider.
 126 The user queries the model through the cloud service. The cloud service provider is equipped with a
 127 trusted CPU TEE (e.g., Intel SGX) that serves as the root of trust, and an untrusted accelerator (e.g.,
 128 GPU) that performs heavy computations but is not fully trustworthy.

129 An ideal protection scheme should satisfy the following security properties:
 130

- **Data Privacy:** The cloud server cannot learn any information about the input x .
- **Model Privacy:** The cloud server cannot learn any information about the model F .
- **t-Integrity:** The probability that a user accepts an incorrect output $\tilde{y} \neq F(x)$ from the cloud
 134 server without aborting is less than t .

135 We treat the CPU TEE as the secure and reliable root of trust (Tramer & Boneh, 2018; Hashemi et al.,
 136 2021), which can be verified through remote attestation. Our goal is to extend these guarantees to
 137 outsourced computations executed on the untrusted accelerator.
 138

139 We note that Intel SGX and other TEEs have been shown vulnerable to side-channel attacks and
 140 denial-of-service attacks (Van Bulck et al., 2018; Van Schaik et al., 2019). These attacks have
 141 been extensively studied, and a wide range of defense mechanisms have been proposed, including
 142 constant-time implementations, oblivious memory primitives, and obfuscation techniques that
 143 conceal both code and data access patterns (Brasser et al., 2019; Lou et al., 2021; Ahmad et al., 2019;
 144 Wichelmann et al., 2024). Such defenses are orthogonal to the focus of this work, which addresses
 145 different aspects of secure computation.

3 BACKGROUND AND RELATED WORK

3.1 TRANSFORMER-BASED FOUNDATION MODELS

151 Transformer architectures (Vaswani et al., 2017) have become the backbone of modern AI, achieving
 152 state-of-the-art performance in natural language processing (Myers et al., 2024), computer vision,
 153 and multi-modal tasks (Awais et al., 2025). Building on this architecture, large-scale foundation
 154 models such as LLaMA (Touvron et al., 2023), Qwen (Yang et al., 2025) and Phi (Abdin et al.,
 155 2024) have emerged, with billions of parameters and pretraining on massive corpora. These models
 156 demonstrate strong generalization and transferability, enabling deployment across diverse applica-
 157 tions, including dialogue systems, code generation, healthcare, and finance. The Attention is the
 158 core module of the Transformer architecture, which can be formulated as:
 159

$$X_l = \text{Attention}(Q, K, V) = \text{SoftMax}(QK^T / \sqrt{d_h})V$$

160 where W are the model parameters with a size of $d_h \times d_h$, and the query, key, and value are computed
 161 via $Q = X_{l-1}W_l^Q$, $K = X_{l-1}W_l^K$, and $V = X_{l-1}W_l^V$.

162 Due to their massive scale, FMs are typically deployed in the cloud, where client inputs may
 163 contain sensitive information and model parameters represent valuable intellectual property. This dual
 164 confidentiality requirement necessitates protecting both user data and proprietary models during in-
 165 ference. To address this challenge, we propose TwinShield, a framework that enables efficient and
 166 secure execution of Transformer-based foundation models with dual protection guarantees.
 167
 168

169 3.2 TRUSTED EXECUTION ENVIRONMENTS (TEEs)

171 Trusted Execution Environments (TEEs) such as Intel SGX provide secure enclaves that guarantee
 172 confidentiality and integrity of computations by isolating code and data from the rest of the system,
 173 including the operating system and hypervisor. These hardware-based protections have motivated
 174 research into running deep learning inference inside TEEs to protect sensitive user data and pro-
 175 prietary models. However, the high computational and memory demands of modern foundation
 176 models make TEE inference inefficient, motivating the use of accelerators such as GPUs to improve
 177 performance.

178 **Limitations of Accelerators with TEEs.** Most current AI infrastructures and cloud platforms lack
 179 TEE-based accelerators, as extending accelerator support remains vendor-specific, technically chal-
 180 lenging, and fraught with unresolved security concerns. Recent studies show that even NVIDIA
 181 H100 GPUs with confidential mode fall short of the security guarantees offered by CPU-based
 182 TEEs, underscoring the need for further refinement of secure accelerator designs (Gu et al., 2025;
 183 Mohan et al., 2024). In addition, many data centers still rely on legacy GPUs, such as A100s and
 184 V100s, making it necessary to explore how these widely deployed accelerators can perform confi-
 185 dential computing. A common approach is to treat the CPU TEE as the root of trust and offload
 186 heavy linear operations to untrusted accelerators through controlled interfaces. Yet, existing proto-
 187 cols cannot simultaneously protect both inputs and model weights, and have been demonstrated only
 188 on small-scale models such as CNNs. Extending secure support to key primitives in Transformer-
 189 based FMs, particularly the attention mechanism, remains a pressing and unresolved challenge.
 190
 191

192 3.3 RELATED WORK

193 We compare TwinShield with several lines
 194 of related work in Table 1. The first cate-
 195 gory executes all computations inside TEEs,
 196 with representative work such as Occlu-
 197 mency (Lee et al., 2019). While this ap-
 198 proach guarantees strong security, it suffers
 199 from significant efficiency loss due to the lim-
 200 ited computational resources available within
 201 TEEs. The second category focuses on pro-
 202 tecting user input data while outsourcing lin-
 203 ear operations to untrusted hardware. Repre-
 204 sentative examples include Slalom (Tramer &
 205 Boneh, 2018) and DarKnight (Hashemi et al.,
 206 2021), which assume that the model belongs
 207 to the cloud provider and therefore do not
 208 address model confidentiality. A third category of work, mainly in on-device scenarios (e.g.,
 209 SOTER (Shen et al., 2022), ShadowNet (Sun et al., 2023), and others (Zhou et al., 2023; Zhang
 210 et al., 2023; Liu et al., 2023; Zhang et al., 2022; Sun et al., 2025; Zhang et al., 2024)), shifts the
 211 focus to model privacy while assuming user inputs remain local and thus unprotected. Since these
 212 protocols do not protect input privacy during computation, they are not applicable to cloud FM
 213 inference setting.

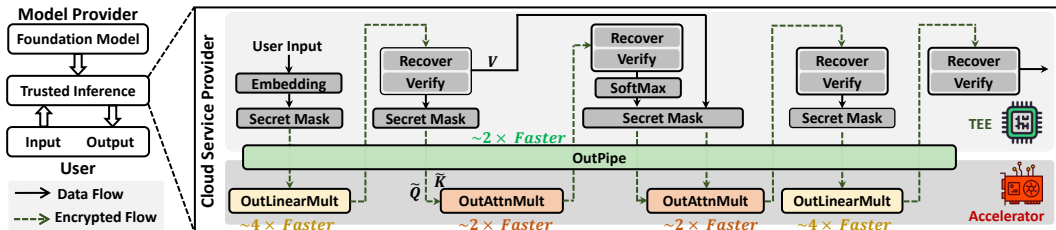
214 Our work, TwinShield, is the first framework designed for dual protection of model and input in
 215 the cloud setting. Moreover, it is the first to efficiently support large-scale FM inference with both
 secure outsourcing of attention computations and optimized TEE-accelerator communication, two
 challenges unique to FM inference that prior approaches did not address.

191 Table 1: OutSrc. stands for outsource and Cld Infer.
 192 for cloud inference. • denotes supported, ○ denotes
 193 not supported, ★ denotes the user input privacy is
 194 protected by on-device setting.

Method	Model Privacy	Input Privacy	Inference Integrity	Linear OutSrc.	Attn OutSrc.	Comm. Optim.	FMs Cld Infer.
Occlumency	•	•	•	○	○	○	○
Slalom	○	•	•	•	○	○	○
DarKnight	○	•	•	•	○	○	○
SOTER	•	★	•	•	○	○	○
ShadowNet	•	★	•	•	○	○	○
NNSplitter	•	○	○	•	○	○	○
TSDP	•	★	○	•	○	○	○
GroupCover	•	★	•	•	○	○	○
TwinShield	•	•	•	•	•	•	•

216 4 TwinShield DESIGN

218 Figure 2 provides an overview of TwinShield, our proposed framework for secure inference. Since
 219 the majority of the computation in Transformer-based Foundation Models comes from large-scale
 220 matrix multiplications (Hoffmann et al., 2022), we propose OutMult which includes OutAttnMult
 221 (in Sec. 4.1) and OutLinearMult (in Sec. 4.2). Then, we propose OutPipe in Sec. 4.2 to overlap
 222 computation and communication, further improving throughput. By outsourcing these bottlenecks,
 223 we can significantly improve overall efficiency and enable secure Transformer inference at scale.



232 Figure 2: Overview of TwinShield. The model developer deploys a foundation model to the cloud
 233 service provider, which hosts a trusted CPU TEE and an untrusted accelerator. The user submits
 234 input to the trusted TEE, which masks sensitive inputs and model parameters before outsourcing
 235 heavy computations to the untrusted accelerator. We propose three secure outsourcing protocols:
 236 OutLinearMult for linear layers, OutAttnMult for attention operations, and OutPipe for pipelined
 237 communication and computation.

238 4.1 OUTSOURCE ATTENTION OPERATION: OutAttnMult

240 Unlike linear operations between weights and inputs, Attention in FMs involves two variable
 241 operands, namely the multiplications between Q and K^T , and between $\text{SoftMax}(QK^T)$ and V .
 242 This variability prevents TEEs from precomputing masked products, as done in prior work (Tramer
 243 & Boneh, 2018; Hashemi et al., 2021; Sun et al., 2023), since the operands are not known before
 244 inference. Consider the multiplication QK^T : the TEE masks Q with R_Q and K^T with R_K^T , and
 245 outsources $(Q + R_Q)(K^T + R_K^T)$ to the accelerator. The result expands to

$$QK^T + R_QK^T + QR_K^T + R_QR_K^T$$

246 To recover QK^T , the TEE must subtract the additional terms. Among them, only $R_QR_K^T$ is pre-
 247 computable, since the other terms depend on the unknown matrices Q or K^T .

248 We observe that the un-precomputable terms, QR_K^T and R_QK^T , each involves one predetermined
 249 mask, which seems to allow outsourcing through precomputation. For example, the TEE could
 250 outsource $(Q + R_Q) \cdot R_K^T$ and then recover QR_K^T by subtracting the precomputed $R_QR_K^T$. However,
 251 this naïve strategy compromises security: exposing R_K^T enables the accelerator adversary to infer
 252 K^T by simply subtracting it from the masked value $K^T + R_K^T$ in the first outsourcing round.

253 To prevent this risk, we propose a *Scale-then-Permute* strategy. Rather than exposing R_K^T directly,
 254 the TEE embeds $R_K^T B$ into the masked matrix $K^T + R_K^T$ with a column-wise permutation, where
 255 B is a scalar matrix. This achieves two goals: (i) it hides the distinction between $K^T + R_K^T$ and
 256 $R_K^T B$, so an attacker cannot recover K^T by simple subtraction without knowing the secret B ; and
 257 (ii) it allows the accelerator to compute $(Q + R_Q)(K^T + R_K^T)$ and $(Q + R_Q)R_K^T B$ in a single round,
 258 avoiding extra communication. The TEE en restores QR_K^T by applying the inverse permutation and
 259 scaling with B^{-1} , and subtracting $R_QR_K^T$. An analogous construction applies symmetrically to R_Q .

260 **Workflow and Complexity Analysis.** The OutAttnMult protocol, illustrated in Figure 3, proceeds
 261 in two phases. In the *offline* phase, the TEE samples masks R_Q and R_K , and generates their scaled
 262 variants using diagonal matrices A and B . In the *online* phase, the TEE embeds and permutes
 263 the masked inputs to construct $\tilde{Q} \in \mathbb{F}^{2m \times n}$ and $\tilde{K}^T \in \mathbb{F}^{n \times 2p}$ with additions and permutations of
 264 cost $O(mn + np)$. The accelerator then performs the dominant multiplication $\tilde{Q}\tilde{K}^T$. Finally, the
 265 TEE recovers the result using four scalings and five additions, also bounded by $O(mn + np)$. In
 266 summary, OutAttnMult reduces the TEE workload from $\mathcal{O}(mnp)$ multiplications to only $\mathcal{O}(mn +$
 267 $np)$ lightweight scalar operations, while offloading the $\mathcal{O}(mnp)$ multiplication to the accelerator.

270 **Security Analysis.** We model the accelerator as an adversary \mathcal{A} interacting with a TEE oracle \mathcal{O} .
 271 For each query, \mathcal{O} returns $\tilde{Q} = \text{perm}(Q + R_Q, AR_Q; \lambda_Q)$ and $\tilde{K}^T = \text{perm}(K^T + R_K^T, R_K^T B; \lambda_K)$,
 272 where masks, scalings, and permutations are secret. Since $Q + R_Q$ forms a one-time pad (Bellare &
 273 Rogaway, 2001), its distribution is indistinguishable from AR_Q in the adversary’s view, while the
 274 scale-then-permuted embedding of $R_K^T B$ prevents subtraction attacks on K^T . Thus, no adversary
 275 running in probabilistic polynomial time (PPT) can recover Q with non-negligible advantage. The
 276 security level can be estimated as $\log_2(\binom{2^m}{m} m! |\mathbb{F}|^m)$ (scalar 8-bit, i.e., $|\mathbb{F}| = 2^\ell$ with $\ell = 8$); for
 277 a typical input length $m = 512$, this is $\approx 8,990$ bits, far exceeding 128/256-bit security; further
 278 details appear in Appendix D.

TEE	Accelerator
Offline:	
<i>Sample:</i>	
$R_Q \leftarrow F^{m \times n}; R_K^T \leftarrow F^{n \times p}; A = \text{diag}(a_1, \dots, a_m), B = \text{diag}(b_1, \dots, b_p)$	
Precompute:	
$AR_Q, R_K^T B$	# TEE Scaler Multiplication
● Embedded Outsource	
$\tilde{Q} = \text{perm}\left(\begin{bmatrix} Q + R_Q \\ AR_Q \end{bmatrix}, \lambda_Q\right)$	→ \tilde{Q}
$\tilde{K}^T = \text{perm}([K^T + R_K^T, R_K^T B], \lambda_K)$	→ \tilde{K}^T
$\text{perm}(\tilde{Q}\tilde{K}^T, \lambda_Q^{-1}, \lambda_K^{-1}) = \begin{bmatrix} T_1, T_2 \\ T_3, T_4 \end{bmatrix}$	← $\tilde{Q}\tilde{K}^T = \tilde{Q} \cdot \tilde{K}^T$
$= \begin{bmatrix} (Q + R_Q)(K^T + R_K^T), (Q + R_Q)R_K^T B \\ AR_Q(K^T + R_K^T), AR_Q R_K^T B \end{bmatrix}$	
● Recovery	
$R_Q R_K^T = A^{-1} \cdot T_4 \cdot B^{-1}$	# TEE Scaler Multiplication
$QR_K^T = T_2 \cdot B^{-1} - R_Q R_K^T$	# TEE Scaler Multiplication and Addition
$R_Q K^T = A^{-1} \cdot T_3 - R_Q R_K^T$	# TEE Scaler Multiplication and Addition
$QK^T = T_1 - R_Q R_K^T - QR_K^T - R_Q K^T$	# TEE Scaler Addition

Figure 3: Protocol of OutAttnMult.

TEE	Accelerator
Offline:	
<i>Sample:</i>	
$R_W \leftarrow F^{m \times n}; R_X \leftarrow F^{n \times p}; C = \text{diag}(c_1, \dots, c_m)$	
Precompute:	
WR_X	
● Embedded Outsource	
$\tilde{W} = \text{perm}\left(\begin{bmatrix} W + R_W \\ CR_W \end{bmatrix}, \lambda_W\right)$	→ \tilde{W}
$\tilde{X} = \text{perm}([X + R_X], \lambda_X)$	→ \tilde{X}
$\text{perm}(\tilde{W}\tilde{X}, \lambda_W^{-1}, \lambda_X^{-1}) = \begin{bmatrix} T_1 \\ T_2 \end{bmatrix}$	← $\tilde{W}\tilde{X} = \tilde{W} \cdot \tilde{X}$
$= \begin{bmatrix} (W + R_W)(X + R_X), (W + R_W)R_X \\ CR_W(X + R_X) \end{bmatrix}$	
● Recovery	
$WX = T_1 - C^{-1} \cdot T_2 - WR_X$	
# TEE Scaler Multiplication and Addition	

Figure 4: Protocol of OutLinearMult.

4.2 OUTSOURCE LINEAR OPERATIONS: OutLinearMult

301 Existing outsourcing schemes such as Slalom (Tramer & Boneh, 2018) protect only the input in
 302 linear computations $Y = WX$: the TEE blinds X with a random mask R_X and precomputes WR_X
 303 offline before outsourcing $(X + R_X)W$. This ensures input privacy but leaves the weight matrix W
 304 exposed, i.e., no dual protection. A natural extension is to also mask the weights by $W + R_W$, so
 305 the accelerator computes $(W + R_W)(X + R_X)$, and the TEE recovers WX by subtracting WR_X ,
 306 $R_W X$, and $R_W R_X$. However, as in attention outsourcing, $R_W X$ cannot be precomputed since X
 307 is unknown before inference. One option is to reuse the OutAttnMult protocol, but the linear case
 308 is simpler because W is known in advance. This allows us to design a more lightweight protocol,
 309 OutLinearMult (in Figure 4). Here, the TEE integrates R_W with $W + R_W$ via a *Scale-then-Permute*
 310 strategy, analogous to handling R_Q and $Q + R_Q$ in OutAttnMult while precomputable terms such
 311 as WR_X are handled offline.

312 **Workflow and Complexity Analysis.** As shown in Figure 4, the protocol proceeds in two phases.
 313 In the *offline* phase, the TEE samples a weight mask $R_W \in \mathbb{F}^{m \times n}$ and an input mask $R_X \in \mathbb{F}^{n \times p}$,
 314 selects a diagonal scalar matrix $C \in \mathbb{F}^{m \times m}$, and precomputes WR_X and CR_W . In the *online* phase,
 315 the TEE masks and permutes the inputs to obtain $\tilde{W} \in \mathbb{F}^{2m \times n}$ and $\tilde{X} \in \mathbb{F}^{n \times p}$, and outsources them
 316 to the accelerator. The accelerator then performs the dominant multiplication $\tilde{W}\tilde{X}$ with complexity
 317 $\mathcal{O}(mnp)$. Finally, in the recovery stage, the TEE applies one scaling and a few additions, with total
 318 cost $\mathcal{O}(mp)$. Altogether, OutLinearMult reduces the TEE workload from $\mathcal{O}(mnp)$ multiplications
 319 in vanilla secure linear computation to only $\mathcal{O}(mn + mp)$ lightweight operations, while offloading
 320 the main $\mathcal{O}(mnp)$ cost to the accelerator.

321 **Security Analysis.** Similar to the protocol of OutAttnMult, we defer the details to the Appendix D.

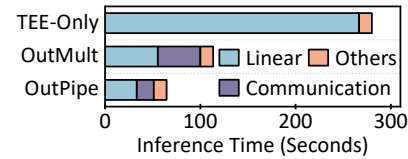
322 **t-Integrity Guarantee.** Following Slalom (Tramer & Boneh, 2018), TwinShield verifies out-
 323 sourced multiplications using Freivalds’ algorithm (Freivalds, 1977). Given matrices A, B and a
 candidate result C , the TEE samples a random vector s and checks whether $Cs = A(Bs)$. If

$C \neq AB$, the probability of passing is at most $1/|\mathbb{F}|$, which drops to $t = (1/|\mathbb{F}|)^k$ after k repetitions. Each check costs only $O(n^2)$, much cheaper than recomputing the $O(n^3)$ product inside the TEE, thus providing efficient and tunable t-Integrity for outsourced linear operations.

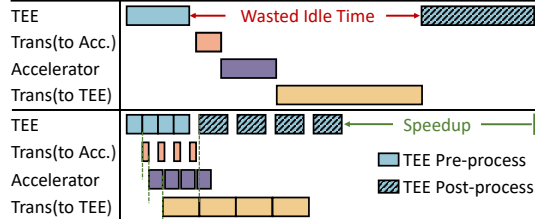
328 4.3 OUTSOURCE COMMUNICATION-COMPUTATION OPTIMIZATION: OutPipe

330 Existing TEE offloading schemes adopt a *serial workflow*: inputs are transferred to the ac-
 331 celerator, computation is performed, and results are copied back to TEE for post-processing.
 332 This design was acceptable for small models such as CNNs, however, foundation models with
 333 billions of parameters impose significant communication overhead. As shown in
 334 Figure 5, after outsourcing linear and attention computations via OutMult, the bottleneck
 335 shifts from computation to communication. This arises because in the *serial workflow*,
 336 the TEE must wait for all accelerator results (and vice versa) before proceeding, leaving
 337 both sides idle during transfers.
 338 As demonstrated in Figure 6 (upper), the TEE remains idle during data transfers and accelerator
 339 computation.

340 To address this challenge, we propose OutPipe, a pipelined workflow that overlaps com-
 341 munication and computation to eliminate the idle time of the serial design. The key ob-
 342 servation is that workloads such as multi-head attention exhibit independence across heads,
 343 which we group into compute blocks. Each block proceeds through four pipeline stages:
 344 preparation inside the TEE, data transfer from TEE to accelerator, computation on the ac-
 345 celerator, and data transfer back to the TEE. This design leverages accelerators that sup-
 346 port concurrent copy-and-compute (NVIDIA, 2025; AMD, 2025). To coordinate the TEE
 347 and the accelerator, we organize their communication through a shared ring buffer divided
 348 into slots. Each slot holds one compute block together with a state flag (READY or DONE).
 349 The TEE fills a free slot and marks it READY, while the accelerator processes ready slots and
 350 marks them DONE once finished. This mechanism decouples the two sides: the TEE can
 351 continue preparing the next block without waiting, and the accelerator can continuously fetch
 352 new work. As shown in Figure 6 (bottom), the pipelined design achieves fine-grained over-
 353 lap across TEE pre-processing, communication, accelerator computation, and TEE post-
 354 processing. Once the TEE finishes pre-
 355 processing the first block, it immediately starts
 356 transferring it to the accelerator while continuing to prepare the next block. Once the first block
 357 arrives, the accelerator begins computation in parallel with the ongoing transfer of the second block.
 358 When the accelerator completes a block, the results are directly transferred back to the TEE while
 359 the accelerator proceeds with the next computation. This staged handoff ensures that all components
 360 (TEE, communication channels, and accelerator) remain active simultaneously, thereby maximizing
 361 utilization and throughput.



362 Figure 5: Inference Breakdown.



363 Figure 6: Comparison of baseline (upper) and pro-
 364 posed OutPipe (bottom).

365 5 EXPERIMENTAL METHODOLOGY

366 In this section, we introduce the experimental methodology.

367 **Models.** We evaluate our approach on four models from three LLM families: LLaMA3 (3B and 8B),
 368 Qwen3 (14B), and Phi-4 (14B). In addition to these LLMs, we also include two vision-language
 369 models, Qwen2.5-VL (7B) and Pixtral (12B) to cover multimodal tasks.

370 **System Setup and Implementation.** We conducted the TwinShield implementation on a server
 371 equipped with an Intel(R) Xeon(R) Gold 6342 CPU running at 2.8GHz and 512GB DRAM, together
 372 with an NVIDIA A40 GPU with 48GB VRAM. TEE enclave is built on the Gramine LibOS, which
 373 runs unmodified applications inside Intel SGX. Communication between TEE and the accelerator is

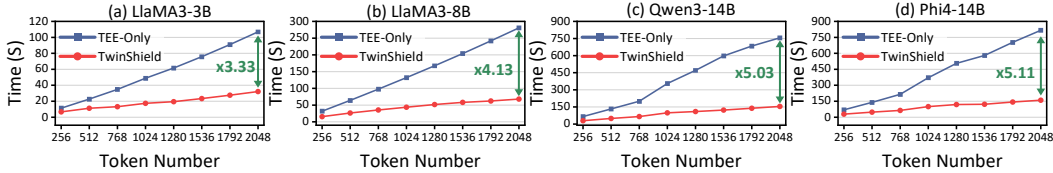
378 enabled via a shared memory region, with EDMM (Enclave Dynamic Memory Management) activated to support dynamic enclave resizing and thread management. Since our threat model excludes
 379 denial-of-service attacks, we assume reliable communication between the CPU and the accelerator.
 380 Furthermore, our matrix computation and model inference framework builds upon `ggml` and
 381 `llama.cpp`, which provide an efficient and lightweight large language model inference pipeline.
 382

383 **Quantization.** TwinShield adopts a quantization strategy for both activations and model weights,
 384 drawing on the approaches of Slalom Tramer & Boneh (2018) and DarKnight Hashemi et al. (2021).
 385 Specifically, it converts values from floating-point to fixed-point by selecting a fractional bit number
 386 l (we use $l = 8$ in our implementation), scaling values by 2^l , and rounding to integers. For negative
 387 values, a correction p is applied to adjust them into the field \mathbb{Z}_p , where the prime is chosen as $p =$
 388 $2^{24} - 3$. The TEEs then outsource the subsequent computations to the GPUs, and later dequantize
 389 the results to recover the original values.
 390

391 6 EXPERIMENTAL RESULTS

393 6.1 END-TO-END PERFORMANCE

395 **Comparison with baseline methods.** We evaluate the proposed TwinShield and TEE-only base-
 396 line (Hanzlik et al., 2021) across four large-scale foundation models, including LLaMA3-3B,
 397 LLaMA3-8B, Qwen3-14B and Phi4-14B. To ensure fairness, both methods are tested under the
 398 same setting, using identical models and adopting the same quantization scheme. As shown in Fig-
 399 ure 7, TwinShield consistently outperforms the TEE-only baseline across different pre-filling token
 400 lengths. For LLaMA3-3B, TwinShield achieves a $3.33\times$ speedup at 2,048 tokens, while the gains
 401 increase to $4.13\times$ for LLaMA3-8B, $5.03\times$ for Qwen3-14B, and $5.11\times$ for Phi4-14B. These results
 402 demonstrate that the benefit of TwinShield scales with model size, effectively reducing the overhead
 403 of secure inference from hundreds of seconds to a fraction of the baseline.
 404



410 Figure 7: Prefilling latency comparison between TEE-only and TwinShield across four foundation
 411 models under varying token lengths. TwinShield consistently achieves multi-fold speedups, with
 412 gains increasing alongside model size and input token lengths.
 413

414 We further compare TwinShield with related outsourcing
 415 methods, Slalom (Tramer & Boneh, 2018) and ShadowNet (Sun et al., 2023), on matrix multiplication. As shown
 416 in Figure 8, TwinShield delivers comparable or better performance while providing dual protection, whereas Slalom
 417 protects only inputs and ShadowNet protects only weights.
 418 The advantage of TwinShield stems from its combination of
 419 protocol-level outsourcing and the pipelined design OutPipe,
 420 which overlaps computation and communication to reduce idle
 421 time and achieve higher throughput.
 422

424 **Results on long-token inputs.** Figure 7 further reports the speedup of TwinShield over the TEE-
 425 only baseline across different token lengths. The relative gain grows with input length; for instance,
 426 on Phi4-14B the speedup increases from $2.42\times$ at shorter inputs to $5.11\times$ at longer ones. This trend
 427 is consistent with our complexity analysis: in the TEE-only baseline, the enclave must perform
 428 the full $\mathcal{O}(mnp)$ multiplications, whereas TwinShield offloads these $\mathcal{O}(mnp)$ operations to the
 429 accelerator and leaves only $\mathcal{O}(mn + mp)$ lightweight scaling and additions in the TEE. As the token
 430 length p increases, the gap between these complexities widens, producing larger speedups.
 431

Model Performance. Our outsourcing protocols do not introduce performance drops, since we
 only offload heavy matrix multiplication to accelerators and the correctness is verified inside the

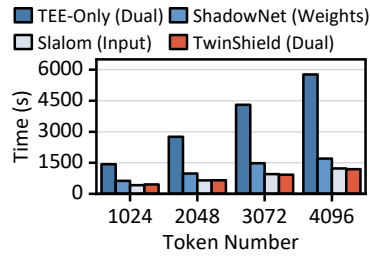


Figure 8: Compare to baselines.

TEE. Thus, the model performance remains identical to the TEE-only baseline. The only source of performance degradation comes from quantization. We therefore measure perplexity (PPL) using the Wikitext (Merity et al., 2016) dataset to quantify this effect. As shown in Table 3, quantization introduces only marginal increases in PPL, while preserving the performance of FMs and enabling efficient secure execution.

Evaluation on vision language models To demonstrate the generality of our method across transformer-based FMs, we further test it on vision-language models (VLMs). Compared to LLMs, VLMs only introduce additional visual tokens while the overall processing pipeline remains identical. We evaluate our approach on Qwen2.5-VL-7B and Pixtral-12B, measuring the runtime for processing image inputs with prompts. Specifically, the input images all have the resolution of 960×619 , which is tokenized into 805 and 2378 tokens. On the other hand, the input text is “Please describe this image in detail”, which is tokenized into 16 and 11 tokens. The inference time and speedups are shown in Table 2.

Table 2: Time and speedup on VLMs.

	T-Vision	T-Text	TEE-Only	TwinShield
Qwen2.5VL-7B	805	16	191.3 s 1.00×	61.2 s 3.13×
Pixtral-12B	2378	11	587.1 s 1.00×	183.9 s 3.19×

Table 3: Quantization effect on Perplexity.

	Original	Quantized
LLaMA3-3B	10.27	10.63
LLaMA3-8B	7.14	7.84
Qwen3-14B	8.42	8.67
Phi4-14B	6.31	6.40

6.2 ABLATION STUDY AND BENCHMARK

Ablation study on the effectiveness of proposed techniques. Figure 9 (a) evaluates the contribution of different components of TwinShield on the Llama3-8B model. By outsourcing all multiplications through OutAttnMult and OutLinearMult, TwinShield achieves $2.71 \times$ inference speedup. Building on this, the system-level optimization OutPipe further enhances the speedup to $4.13 \times$ by overlapping TEE preparation, communication, and accelerator computation. This overlap eliminates the idle periods inherent in the serial workflow, thereby improving utilization on both the TEE and the accelerator and delivering substantial end-to-end performance gains.

Performance Evaluation on Micro-Benchmark. To isolate the effect of the protocol itself, we benchmark the matrix multiplications in Attention independently. Figure 9 (b) shows that OutAttnMult accelerates these operations, and with OutPipe reduces latency by $2.4 \times$ at 2048 tokens. For linear layers, OutLinearMult with OutPipe achieves a $4.2 \times$ reduction at the same length.

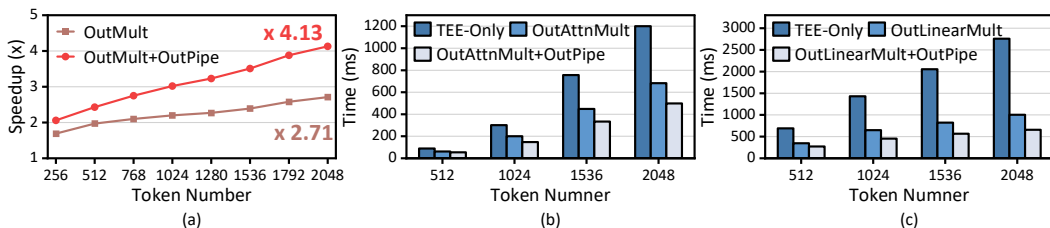


Figure 9: (a) End-to-end improvements with different techniques. OutMult includes OutAttnMult and OutLinearMult. (b) Latency of Attention Multiplication. (c) Latency of Linear Multiplication.

7 CONCLUSION

We propose TwinShield, a framework for secure and efficient foundation model inference that unifies TEEs with crypto-protected accelerators. By introducing OutAttnMult, OutLinearMult, and the pipelined scheme OutPipe, TwinShield achieves dual protection of inputs and models while enabling lightweight integrity verification. Experiments across multiple large-scale models show up to $5.03 \times$ speedup over TEE-only execution, with ablation and micro-benchmarks confirming the complementary benefits of protocol- and system-level optimizations. These results demonstrate that TwinShield effectively bridges the gap between security and efficiency, offering a practical path toward trustworthy Foundation Model-as-a-Service.

486 REFERENCES
487

488 Marah Abdin, Jyoti Aneja, Harkirat Behl, Sébastien Bubeck, Ronen Eldan, Suriya Gunasekar,
489 Michael Harrison, Russell J Hewett, Mojan Javaheripi, Piero Kauffmann, et al. Phi-4 techni-
490 cal report. *arXiv preprint arXiv:2412.08905*, 2024.

491 Adil Ahmad, Byunggill Joe, Yuan Xiao, Yinqian Zhang, Insik Shin, and Byoungyoung Lee. Obfus-
492 curo: A commodity obfuscation engine on intel sgx. In *Network and Distributed System Security*
493 *Symposium*, 2019.

494 AMD. Hip developing guide. [https://rocm.docs.amd.com/projects/HIP/en/](https://rocm.docs.amd.com/projects/HIP/en/docs-develop/)
495 docs-develop/, 2025.

496 Muhammad Awais, Muzammal Naseer, Salman Khan, Rao Muhammad Anwer, Hisham Cholakkal,
497 Mubarak Shah, Ming-Hsuan Yang, and Fahad Shahbaz Khan. Foundation models defining a
498 new era in vision: a survey and outlook. *IEEE Transactions on Pattern Analysis and Machine*
499 *Intelligence*, 2025.

500 Mihir Bellare and Phillip Rogaway. Introduction to modern cryptography. *Lecture Notes*, 2001.

501 Ferdinand Brasser, Srdjan Capkun, Alexandra Dmitrienko, Tommaso Frassetto, Kari Kostainen, and
502 Ahmad-Reza Sadeghi. Dr. sgx: Automated and adjustable side-channel protection for sgx using
503 data location randomization. In *Proceedings of the 35th Annual Computer Security Applications*
504 *Conference*, pp. 788–800, 2019.

505 Jack Choquette. Nvidia hopper h100 gpu: Scaling performance. *IEEE Micro*, 43(3):9–17, 2023.

506 Ronald Cramer, Ivan Bjerre Damgård, et al. *Secure multiparty computation*. Cambridge University
507 Press, 2015.

508 Daniel Demmler, Thomas Schneider, and Michael Zohner. Aby-a framework for efficient mixed-
509 protocol secure two-party computation. In *NDSS*, 2015.

510 Jacob Devlin, Ming-Wei Chang, Kenton Lee, and Kristina Toutanova. Bert: Pre-training of deep
511 bidirectional transformers for language understanding. *arXiv preprint arXiv:1810.04805*, 2018.

512 Alexey Dosovitskiy, Lucas Beyer, Alexander Kolesnikov, Dirk Weissenborn, Xiaohua Zhai, Thomas
513 Unterthiner, Mostafa Dehghani, Matthias Minderer, Georg Heigold, Sylvain Gelly, et al. An
514 image is worth 16x16 words: Transformers for image recognition at scale. *arXiv preprint*
515 *arXiv:2010.11929*, 2020.

516 Rusins Freivalds. Probabilistic machines can use less running time. In *IFIP congress*, volume 839,
517 pp. 842, 1977.

518 Zhongshu Gu, Enriquillo Valdez, Salman Ahmed, Julian James Stephen, Michael Le, Hani
519 Jamjoom, Shixuan Zhao, and Zhiqiang Lin. Nvidia gpu confidential computing demystified.
520 *arXiv preprint arXiv:2507.02770*, 2025.

521 Lucjan Hanzlik, Yang Zhang, Kathrin Grosse, Ahmed Salem, Maximilian Augustin, Michael
522 Backes, and Mario Fritz. Mlcapsule: Guarded offline deployment of machine learning as a ser-
523 vice. In *Proceedings of the IEEE/CVF conference on computer vision and pattern recognition*,
524 pp. 3300–3309, 2021.

525 Hanieh Hashemi, Yongqin Wang, and Murali Annavaram. Darknight: An accelerated framework
526 for privacy and integrity preserving deep learning using trusted hardware. In *MICRO-54: 54th*
527 *Annual IEEE/ACM International Symposium on Microarchitecture*, pp. 212–224, 2021.

528 Jordan Hoffmann, Sebastian Borgeaud, Arthur Mensch, Elena Buchatskaya, Trevor Cai, Eliza
529 Rutherford, Diego de Las Casas, Lisa Anne Hendricks, Johannes Welbl, Aidan Clark, et al. Train-
530 ing compute-optimal large language models. *arXiv preprint arXiv:2203.15556*, 2022.

531 Intel SGX. Intel® software guard extensions (intel® sgx) developer guide.
532 <https://www.intel.com/content/www/us/en/developer/tools/>
533 software-guard-extensions/overview.html, 2023.

540 Taegyeong Lee, Zhiqi Lin, Saumay Pushp, Caihua Li, Yunxin Liu, Youngki Lee, Fengyuan Xu,
 541 Chenren Xu, Lintao Zhang, and Junehwa Song. Occlumency: Privacy-preserving remote deep-
 542 learning inference using sgx. In *The 25th Annual International Conference on Mobile Computing
 543 and Networking*, pp. 1–17, 2019.

544 Ziyu Liu, Yukui Luo, Shijin Duan, Tong Zhou, and Xiaolin Xu. Mirrornet: A tee-friendly framework
 545 for secure on-device dnn inference. In *2023 IEEE/ACM International Conference on Computer
 546 Aided Design (ICCAD)*, pp. 1–9. IEEE, 2023.

547 Xiaoxuan Lou, Tianwei Zhang, Jun Jiang, and Yinqian Zhang. A survey of microarchitectural side-
 548 channel vulnerabilities, attacks, and defenses in cryptography. *ACM Computing Surveys (CSUR)*,
 549 54(6):1–37, 2021.

550 Stephen Merity, Caiming Xiong, James Bradbury, and Richard Socher. Pointer sentinel mixture
 551 models, 2016.

552 Apoorve Mohan, Mengmei Ye, Hubertus Franke, Mudhakar Srivatsa, Zhuoran Liu, and Nel-
 553 son Mimura Gonzalez. Securing ai inference in the cloud: Is cpu-gpu confidential computing
 554 ready? In *2024 IEEE 17th International Conference on Cloud Computing (CLOUD)*, pp. 164–
 555 175. IEEE, 2024.

556 Devon Myers, Rami Mohawesh, Venkata Ishwarya Chellaboina, Anantha Lakshmi Sathvik, Praveen
 557 Venkatesh, Yi-Hui Ho, Hanna Henshaw, Muna Alhawawreh, David Berdik, and Yaser Jararweh.
 558 Foundation and large language models: fundamentals, challenges, opportunities, and social im-
 559 pacts. *Cluster Computing*, 27(1):1–26, 2024.

560 NVIDIA. *CUDA C++ Programming Guide*. NVIDIA, 2025. URL <https://docs.nvidia.com/cuda/cuda-c-programming-guide/index.html>.

561 T Pahima. Breakingformation: Orca security research team discovers aws cloudformation vulnera-
 562 bility. *Complete Cloud Security in Minutes-Orca Security*, 2022.

563 Tianxiang Shen, Ji Qi, Jianyu Jiang, Xian Wang, Siyuan Wen, Xusheng Chen, Shixiong Zhao, Sen
 564 Wang, Li Chen, Xiapu Luo, et al. {SOTER}: Guarding black-box inference for general neural
 565 networks at the edge. In *2022 USENIX Annual Technical Conference (USENIX ATC 22)*, pp.
 566 723–738, 2022.

567 Tong Sun, Bowen Jiang, Hailong Lin, Borui Li, Yixiao Teng, Yi Gao, and Wei Dong. Tensor-
 568 shield: Safeguarding on-device inference by shielding critical dnn tensors with tee. *arXiv preprint
 569 arXiv:2505.22735*, 2025.

570 Zhichuang Sun, Ruimin Sun, Changming Liu, Amrita Roy Chowdhury, Long Lu, and Somesh Jha.
 571 Shadownet: A secure and efficient on-device model inference system for convolutional neural
 572 networks. In *2023 IEEE Symposium on Security and Privacy (SP)*, pp. 1596–1612. IEEE, 2023.

573 Hugo Touvron, Thibaut Lavril, Gautier Izacard, Xavier Martinet, Marie-Anne Lachaux, Timothée
 574 Lacroix, Baptiste Rozière, Naman Goyal, Eric Hambro, Faisal Azhar, et al. Llama: Open and
 575 efficient foundation language models. *arXiv preprint arXiv:2302.13971*, 2023.

576 Florian Tramer and Dan Boneh. Slalom: Fast, verifiable and private execution of neural networks in
 577 trusted hardware. In *International Conference on Learning Representations*, 2018.

578 L Tung. Google cloud: Here are the six’best’vulnerabilities security researchers found last year.
 579 *ZDNET, Mar*, 2021.

580 Jo Van Bulck, Marina Minkin, Ofir Weisse, Daniel Genkin, Baris Kasikci, Frank Piessens, Mark
 581 Silberstein, Thomas F Wenisch, Yuval Yarom, and Raoul Strackx. Foreshadow: Extracting the
 582 keys to the intel {SGX} kingdom with transient {Out-of-Order} execution. In *27th USENIX
 583 Security Symposium (USENIX Security 18)*, pp. 991–1008, 2018.

584 Stephan Van Schaik, Alyssa Milburn, Sebastian Österlund, Pietro Frigo, Giorgi Maisuradze, Kaveh
 585 Razavi, Herbert Bos, and Cristiano Giuffrida. Ridl: Rogue in-flight data load. In *2019 IEEE
 586 Symposium on Security and Privacy (SP)*, pp. 88–105. IEEE, 2019.

594 Ashish Vaswani, Noam Shazeer, Niki Parmar, Jakob Uszkoreit, Llion Jones, Aidan N Gomez,
 595 Łukasz Kaiser, and Illia Polosukhin. Attention is all you need. *Advances in neural informa-*
 596 *tion processing systems*, 30, 2017.

597

598 Yuntao Wei, Xueyan Wang, Song Bian, Weisheng Zhao, and Yier Jin. The-v: Verifiable privacy-
 599 preserving neural network via trusted homomorphic execution. In *2023 IEEE/ACM International*
 600 *Conference on Computer Aided Design (ICCAD)*, pp. 1–9. IEEE, 2023.

601 Jan Wichelmann, Anja Rabich, Anna Pätschke, and Thomas Eisenbarth. Obelix: Mitigating side-
 602 channels through dynamic obfuscation. In *2024 IEEE Symposium on Security and Privacy (SP)*,
 603 pp. 4182–4199. IEEE, 2024.

604

605 An Yang, Anfeng Li, Baosong Yang, Beichen Zhang, Binyuan Hui, Bo Zheng, Bowen Yu,
 606 Chang Gao, Chengen Huang, Chenxu Lv, et al. Qwen3 technical report. *arXiv preprint*
 607 *arXiv:2505.09388*, 2025.

608

609 Zheng Zhang, Na Wang, Ziqi Zhang, Yao Zhang, Tianyi Zhang, Jianwei Liu, and Ye Wu. Group-
 610 cover: a secure, efficient and scalable inference framework for on-device model protection based
 611 on tees. In *Forty-first international conference on machine learning*, 2024.

612

613 Ziqi Zhang, Lucien KL Ng, Bingyan Liu, Yifeng Cai, Ding Li, Yao Guo, and Xiangqun Chen.
 614 Teeslice: slicing dnn models for secure and efficient deployment. In *Proceedings of the 2nd ACM*
 615 *International Workshop on AI and Software Testing/Analysis*, pp. 1–8, 2022.

616

617 Ziqi Zhang, Chen Gong, Yifeng Cai, Yuanyuan Yuan, Bingyan Liu, Ding Li, Yao Guo, and Xiangqun
 618 Chen. No privacy left outside: On the (in-) security of tee-shielded dnn partition for on-device
 619 ml. In *2024 IEEE Symposium on Security and Privacy (SP)*, pp. 52–52. IEEE Computer Society,
 620 2023.

621

622 Tong Zhou, Yukui Luo, Shaolei Ren, and Xiaolin Xu. Nnsplitter: an active defense solution for dnn
 623 model via automated weight obfuscation. In *Proceedings of the 40th International Conference on*
 624 *Machine Learning*, ICML’23. JMLR.org, 2023.

625

626

627

628

629

630

631

632

633

634

635

636

637

638

639

640

641

642

643

644

645

646

647

648	APPENDIX	
649		
650	A The Use of Large Language Models (LLMs)	14
651		
652	B Ethics statement	14
653		
654	C Reproducibility Statement	14
655		
656	D Security Analysis of OutAttnMult	14
657		
658	D.1 Analysis Takeaway	14
659	D.2 Feasible Set Construction	15
660	D.3 Theoretical guarantee	15
661	D.4 Bounding the adversary’s success probability	16
662	D.5 Discussion	16
663		
664	E Security Analysis of OutLinearMult	16
665		
666	E.1 Theoretical guarantee	16
667	E.2 Bounding the adversary’s success probability	17
668	E.3 Discussion	17
669		
670	F Background and Related Work	17
671		
672	F.1 Transformers	17
673	F.2 Trusted Execution Environments (TEEs)	18
674	F.3 Secret Sharing for Data Confidentiality	19
675	F.4 Computation Verification for Integrity	19
676		
677		
678		
679		
680		
681		
682		
683		
684		
685		
686		
687		
688		
689		
690		
691		
692		
693		
694		
695		
696		
697		
698		
699		
700		
701		

702 A THE USE OF LARGE LANGUAGE MODELS (LLMs)
703704 The authors used ChatGPT and Grammarly to check and correct any typos and grammatical errors.
705706 B ETHICS STATEMENT
707709 This work focuses on improving the security and efficiency of foundation model inference by com-
710 bining TEEs with cryptographic protocols. Our study does not involve human or animal subjects,
711 nor does it require the collection of personal or sensitive data. The evaluation uses publicly avail-
712 able pretrained models and datasets, and no private or proprietary datasets are disclosed. We believe
713 our method enhances privacy protection by safeguarding both user data and model confidentiality in
714 cloud inference. The research complies with the ICLR Code of Ethics, and we are not aware of any
715 ethical concerns or potential harms arising from this work.
716717 C REPRODUCIBILITY STATEMENT
718719 We have taken multiple steps to ensure the reproducibility of our work. The code is publicly avail-
720 able at <https://anonymous.4open.science/r/Twinshield>, together with a README file that includes
721 instructions for installation, configuration, and execution of experiments.
722724 D SECURITY ANALYSIS OF OutAttnMult
725726 D.1 ANALYSIS TAKEAWAY
727728 In the outsourcing protocol in Figure 3, data inside the TEE is protected, while data processed by the
729 accelerator may be observed by adversaries. To prevent attackers from inferring the original Q , the
730 TEE constructs a masked representation \tilde{Q} by (i) adding a random mask R_Q , (ii) permuting $Q + R_Q$
731 together with AR_Q under secret permutation indices, and (iii) scaling rows with a private diagonal
732 matrix A .
733From the adversary’s perspective, recovering Q from \tilde{Q} requires solving three layers of uncertainty:
734735 1. Combination: choosing which m out of the $2m$ rows correspond to the true $Q + R_Q$ block,
736 contributing $\binom{2m}{m}$ possibilities.
737 2. Permutation: recovering the correct order of these m rows, contributing $m!$ possibilities.
738 3. Scaling: guessing the diagonal scaling applied to each row, with each entry selected from
739 the finite field \mathbb{F} , contributing $|\mathbb{F}|^m$ possibilities.
740742 Putting these together, the adversary’s search space is
743

744
$$\binom{2m}{m} \cdot m! \cdot |\mathbb{F}|^m,$$

745

746 and thus the security level is quantified as
747

748
$$\log_2 \left(\binom{2m}{m} m! |\mathbb{F}|^m \right),$$

749

751 where $2m$ denotes the total number of rows in \tilde{Q} and $|\mathbb{F}|$ is the size of the finite field. Here, $\binom{2m}{m}$
752 captures the row combination, $m!$ the permutation order, and $|\mathbb{F}|^m$ the design space of the diagonal
753 matrix A .
754755 For a typical FM setting with input length $m = 512$ and 8-bit scalars (i.e., $|\mathbb{F}| = 2^8$), this evaluates
to roughly 8,990 bits of security, which is far beyond the standard 128/256-bit levels.

756 D.2 FEASIBLE SET CONSTRUCTION
757

758 We formalize the feasible set $\mathcal{F}(\hat{Z})$ of all possible pre-images Z of a transformed and shuffled matrix
759 $\hat{Z} \in \mathbb{R}^{t \times d}$ (here Z represents Q , K , or W). Let n be the number of original rows, $t = |\hat{Z}|$ the total
760 number of rows observed, and $m = t - n$ the number of mask rows. Denote $[t] = \{1, \dots, t\}$ and
761 let \mathcal{D} be the set of admissible non-singular diagonal scaling matrices used by the transformation.
762

763 **Assumption.** Rows in \hat{Z} are generated by concatenating the original and mask rows, applying a
764 common right diagonal scaling $D \in \mathcal{D}$, followed by a row permutation; i.e.,
765

$$766 \hat{Z} = \Pi [Z; R] D,$$

767 where $R = \begin{bmatrix} r_1^\top \\ \vdots \\ r_m^\top \end{bmatrix}$ and Π permute t rows.
768
769
770

771 1. **(Candidate mask index sets)** For any $\Omega \subseteq [t]$ with $|\Omega| = m$, define the candidate mask
772 set
773

$$774 \Phi_\Omega = \{\hat{z}_j^\top \mid j \in \Omega\}, \quad C_\Omega = [t] \setminus \Omega.$$

775 Here \hat{z}_j^\top denotes the j -th row of \hat{Z} .
776

777 2. **(Candidate original rows)** Choose any injective selection $\psi : [n] \hookrightarrow C_\Omega$ and set $\bar{Z} =$
778 $[\bar{z}_1^\top; \dots; \bar{z}_n^\top]$ with $\bar{z}_i^\top = \hat{z}_{\psi(i)}^\top$.
779
780 3. **(Candidate ordering)** For any permutation σ on $[n]$, form $\bar{Z}_\sigma = [\bar{z}_{\sigma(1)}^\top; \dots; \bar{z}_{\sigma(n)}^\top]$.
781
782 4. **(Per-row feasible pre-images)** For each $i \in [n]$, define

$$783 \mathcal{F}_{\Omega, \psi, \sigma}^i(\hat{Z}) = \{z^\top \in \mathbb{R}^d \mid \exists D \in \mathcal{D}, \exists \hat{z}'^\top \in \Phi_\Omega \text{ s.t. } z^\top = (\bar{z}_{\sigma(i)}^\top - \hat{z}'^\top)D^{-1}\}.$$

784 5. **(Matrix-level feasible set)** The feasible set corresponding to (Ω, ψ, σ) is the Cartesian
785 product
786

$$787 \mathcal{F}_{\Omega, \psi, \sigma}(\hat{Z}) = \prod_{i=1}^n \mathcal{F}_{\Omega, \psi, \sigma}^i(\hat{Z}),$$

788 and the global feasible set is
789

$$790 \mathcal{F}(\hat{Z}) = \bigcup_{\Omega \in \binom{[t]}{m}} \bigcup_{\psi} \bigcup_{\sigma} \mathcal{F}_{\Omega, \psi, \sigma}(\hat{Z}).$$

791 Let the obfuscation ratio be $r := m/t$. Under fixed n and a fixed \mathcal{D} , increasing r (equivalently t)
792 strictly enlarges the index-family $\binom{[t]}{m}$ and hence cannot decrease $\mathcal{F}(\hat{Z})$ (monotonicity).
793

794 D.3 THEORETICAL GUARANTEE
795

796 **Assumption (Obfuscation Model).** All computations are carried out over a large finite field \mathbb{F}_p
797 (via fixed-point quantization). TEE samples secret diagonal scalings A, B , secret permutations
798 λ_Q, λ_K , and fresh random mask blocks R_Q, R_K uniformly at random; none are revealed to the
799 GPU. The embedded, permuted inputs are

$$800 \widetilde{Q} = \text{perm}(Q + R_Q, AR_Q; \lambda_Q), \quad \widetilde{K}^T = \text{perm}(K^T + R_K^T, R_K^T B; \lambda_K),$$

801 where $\text{perm}(\cdot, \cdot; \lambda)$ concatenates the two blocks along the embedding dimension and applies per-
802 mutation λ .
803

804 **Theorem 1 (Indistinguishability).** For a $\widetilde{Q}K^T$ computation and GPU view
805

$$806 \text{View}_{\text{GPU}} = (\widetilde{Q}, \widetilde{K}^T, \widetilde{Q}K^T, (QK^T)'),$$

810 where $(QK^T)'$ is freshly re-masked inside the TEE, we have
 811

$$812 \forall (Q_i, Q_j) \in \mathcal{F}(\tilde{Q})^2 : \Pr[Q = Q_i \mid \text{View}_{\text{GPU}}] = \Pr[Q = Q_j \mid \text{View}_{\text{GPU}}], \quad (1)$$

$$813 \forall (K_i^T, K_j^T) \in \mathcal{F}(\tilde{K}^T)^2 : \Pr[K^T = K_i^T \mid \text{View}_{\text{GPU}}] = \Pr[K^T = K_j^T \mid \text{View}_{\text{GPU}}]. \quad (2)$$

815 *Proof sketch.*

817

- 818 • **Lemma 1.** The attacker cannot recover QK^T from $(\tilde{QK}^T, (QK^T)')$ because the TEE
 819 inverts the embeddings with secret $(A, B, \lambda_Q, \lambda_K)$ and then applies fresh re-masking; these
 820 are unknown to the GPU.
- 821 • **Lemma 2.** Masked vectors from R_Q, R_K are indistinguishable from transformed data
 822 vectors: over \mathbb{F}_p , additive masking with fresh uniform vectors (scaled by secret diagonals)
 823 is a one-time pad; permutation hides positions.

824 Together these lemmas imply uniform posterior distributions over feasible sets, proving equa-
 825 tion 1–equation 2.

827 D.4 BOUNDING THE ADVERSARY’S SUCCESS PROBABILITY

829 The chance of exactly recovering (Q, K^T) is bounded by the feasible-set sizes:

$$830 \Pr[\text{Correct}] \leq \frac{1}{|\mathcal{F}(\tilde{Q})| \cdot |\mathcal{F}(\tilde{K}^T)|}. \quad (3)$$

833 Conservative lower bounds are

$$834 |\mathcal{F}(\tilde{Q})| \geq \binom{t_Q}{n_Q} n_Q! (p-1)^{\kappa_Q}, \quad |\mathcal{F}(\tilde{K}^T)| \geq \binom{t_K}{n_K} n_K! (p-1)^{\kappa_K}, \quad (4)$$

837 yielding

$$838 \Pr[\text{Correct}] \leq \left[\binom{t_Q}{n_Q} n_Q! (p-1)^{\kappa_Q} \right]^{-1} \cdot \left[\binom{t_K}{n_K} n_K! (p-1)^{\kappa_K} \right]^{-1}. \quad (5)$$

841 D.5 DISCUSSION

843 Increasing the obfuscation ratio $r = m/t$ enlarges feasible sets, thereby lowering the adversary’s
 844 success probability. Each round uses fresh masks (R_Q, R_K) (and may refresh $A, B, \lambda_Q, \lambda_K$), en-
 845 suring independence across rounds and preventing cumulative leakage.

847 E SECURITY ANALYSIS OF OutLinearMult

849 E.1 THEORETICAL GUARANTEE

851 **Assumption (Obfuscation Model).** All computations take place over \mathbb{F}_p . The TEE samples: (i)
 852 a secret row-wise diagonal scaling $C = \text{diag}(c_1, \dots, c_{d_{\text{out}}})$; (ii) fresh mask rows R_W ; and (iii) a
 853 secret row permutation Π . These are never revealed to the accelerator. The transformed weights and
 854 masked inputs are

$$855 \widetilde{W} = \Pi \begin{bmatrix} W + R_W \\ CR_W \end{bmatrix}, \quad \widetilde{X} = X + R_X,$$

857 with R_X uniform. The accelerator computes $\widetilde{Y} = \widetilde{W} \widetilde{X}$, while the TEE recovers WX using (C, Π)
 858 and offline correction WR_X .

860 **Adversary’s view.** The accelerator observes
 861

$$862 \text{View}_{\text{lin}} = (\widetilde{W}, \widetilde{X}, \widetilde{W} \widetilde{X}, (WX)^\diamond),$$

863 where $(WX)^\diamond$ is freshly re-masked inside the TEE.

864 **Theorem 3 (Indistinguishability).** Conditioned on View_{lin} , all $W' \in \mathcal{F}(\widetilde{W})$ are equally likely:
 865

$$866 \quad \forall (W', W'') \in \mathcal{F}(\widetilde{W})^2 : \quad \Pr[W = W' \mid \text{View}_{\text{lin}}] = \Pr[W = W'' \mid \text{View}_{\text{lin}}]. \quad (6)$$

867 *Proof sketch.*

868

- 869 • **Lemma 3.** Since $\widetilde{X} = X + R_X$ with R_X uniform, \widetilde{X} is information-theoretically inde-
 870 pendent of W .
- 871 • **Lemma 4.** The TEE uses (C, Π) and WR_X to obtain WX , then re-masks it freshly. With
 872 (C, Π, R_W, R_X) secret, the pair $(\widetilde{W}\widetilde{X}, (WX)^\diamond)$ leaks nothing about W .

873 Thus View_{lin} is invariant across feasible pre-images, proving equation 6.

874 E.2 BOUNDING THE ADVERSARY’S SUCCESS PROBABILITY

875 The attacker’s chance of reconstructing W exactly is bounded by

$$876 \quad \Pr[\text{Correct}] \leq \frac{1}{|\mathcal{F}(\widetilde{W})|}. \quad (7)$$

877 A conservative lower bound is

$$878 \quad |\mathcal{F}(\widetilde{W})| \geq \binom{t}{d_{\text{out}}} d_{\text{out}}! (p-1)^\kappa, \quad (8)$$

879 where $t = d_{\text{out}} + m$ is the number of real+mask rows and κ the independent scales in C . Hence

$$880 \quad \Pr[\text{Correct}] \leq \left[\binom{t}{d_{\text{out}}} d_{\text{out}}! (p-1)^\kappa \right]^{-1}. \quad (9)$$

881 E.3 DISCUSSION

882 Monotonicity holds: increasing $r = m/t$ enlarges feasible sets and decreases the adversary’s success
 883 probability. Each round uses fresh (R_X, R_W) (and may refresh (C, Π)), ensuring independence
 884 across layers and preventing cumulative leakage.

885 F BACKGROUND AND RELATED WORK

886 F.1 TRANSFORMERS

887 Transformer architecture consists of an embedding layer and consecutive transformer layers. Every
 888 transformer layer is a composition of a multi-head self-attention (MHA) module, a feed-forward
 889 (FFN) module, two normalization modules and residual connections. The input data is transformed
 890 into a token sequence through the embedding layer with positional encoding. The input token se-
 891 quence can be uniformly denoted as $X_e \in \mathbb{R}^{N \times D}$, where N is the number of tokens and D is the
 892 embedding dimension. We describe the main computation blocks in Transformers below.

893 **Additive Linear Operations.** The additive linear operations in Transformers are mainly the linear
 894 layers, where the output features are computed by multiplying the input features with weight
 895 matrices. In the Attention module, given the input tokens $X_e \in \mathbb{R}^{N \times D}$, the output $Q, K, V \in \mathbb{R}^{N \times D}$ are
 896 computed by multiplying X_e with three weight matrices $W_q, W_k, W_v \in \mathbb{R}^{D \times D}$:

$$897 \quad Q = X_e W_q, \quad K = X_e W_k, \quad V = X_e W_v. \quad (10)$$

898 Similarly, in the Feed Forward module, the embedding $X_e \in \mathbb{R}^{N \times D}$ is multiplied by two weight
 899 matrices $W_1, W_2 \in \mathbb{R}^{D' \times D}$:

$$900 \quad \text{FeedForward}(X_e) = \text{Act}(X_e \cdot W_1^T) \cdot W_2 \quad (11)$$

901 Existing techniques Tramer & Boneh (2018); Hashemi et al. (2021) can securely outsource these
 902 additive linear operations while protecting the input data X_e . However, they cannot protect the
 903 weight matrices W , which remain exposed to the untrusted accelerator.

918 **Multiplicative Attention Operations.** There are massive multiplicative linear operations in Trans-
 919 formers which cannot be outsourced via prior methods. The primary multiplicative attention opera-
 920 tions are computing the attention map and attention output in the Attention module:
 921

$$922 \quad \text{Attention}(Q, K, V) = \text{SoftMax}(QK^T / \sqrt{d_h})V \quad (12)$$

923 The multiplicative operations (e.g., $Q \cdot K^T$) are fundamentally different from the additive linear
 924 operations (e.g., $Q = X_e \cdot W_q$). This is because in the multiplicative operations, neither operand is a
 925 constant matrix. As a result, the multiplicative operations cannot be securely outsourced via existing
 926 techniques. We refer to the matrix multiplication between Q and K , and between the attention map
 927 and V as attention matrix multiplication.

928 The multiplicative linear operations such as $Q \cdot K^T$ are computed independently across multiple
 929 attention heads. For MHA with H heads, the multi-head attention is computed as:
 930

$$931 \quad MHA(Q, K, V) = \text{Concat}(\text{head}_1, \dots, \text{head}_H)W_O \quad (13)$$

932 where $\text{Concat}(\cdot)$ is the concatenation operation,
 933

$$934 \quad \text{head}_i = \text{Attention}(XW_q^i, XW_k^i, XW_v^i) \quad (14)$$

935 and $W_O \in \mathbb{R}^{Hd_h \times D}$ is a weight matrix to map features in all heads to the output dimension. The
 936 MHA is the key mechanism in the Transformers and also the performance bottleneck. However, ex-
 937 isting works cannot securely outsource the heavy computation in the multiplicative linear operations
 938 within the MHA module.

940 F.2 TRUSTED EXECUTION ENVIRONMENTS (TEEs)

941 TEEs like Intel SGX (Intel SGX) provide a secure environment where data confidentiality and,
 942 in some cases, computation integrity are ensured by hardware. Intel SGX specifically safeguards
 943 the confidentiality and integrity by isolating data and code within an enclave, shielded from exter-
 944 nal elements including the operating system, hypervisor, and hardware devices on the system bus.
 945 This isolation involves a dedicated memory region, the Processor Reserved Memory (PRM), man-
 946 aged by SGX-enabled CPUs. Here, the Enclave Page Cache (EPC) stores enclave data and code
 947 in 4 KB pages, accessible only through specific CPU instructions. This setup prevents unautho-
 948 rized access to the EPC, maintaining a secure environment for sensitive computations. SGX also
 949 supports remote attestation, allowing remote verification of an enclave’s integrity through crypto-
 950 graphic proofs. These features have inspired research into running deep learning inference entirely
 951 within CPU TEEs to protect data and model confidentiality (Hanzlik et al., 2021). However, the high
 952 computational and memory demands of deep learning models make CPU TEE inference inefficient,
 953 motivating the use of accelerators such as GPUs, TPUs, and ASICs to improve performance.

954 **TEE with AI Accelerators.** Although some high-end accelerators (e.g., NVIDIA H100 (Choquette,
 955 2023)) have begun to support TEE capabilities, enabling secure computation directly on the accel-
 956 erator remains impractical in most real-world deployments. This is due to two key factors: firstly,
 957 TEE-enabled accelerators are rare and expensive, while many emerging and legacy GPUs (such as
 958 GTX series and A100) currently deployed in data centers remain in use and are likely to persist for
 959 years. Secondly, the growing heterogeneity of hardware accelerators (e.g., GPUs, TPUs, and FP-
 960 GAs) introduces vendor incompatibilities and the complexity of cross-device TEE protocols, making
 961 a unified TEE solution across diverse devices infeasible;

962 For accelerators without native TEE support, a more promising approach treats the CPU TEE as
 963 the root of trust, and considers the accelerator as an untrusted but controlled extension of the TEE.
 964 In this design, sensitive data is decrypted and processed inside the CPU TEE, which enforces strict
 965 isolation and integrity guarantees, while delegating computationally intensive linear operations to
 966 the untrusted accelerator through carefully controlled and isolated interfaces. These interfaces may
 967 include exclusive device assignment, core pinning, and secure memory buffer management to min-
 968 imize the risk of confidential data leakage. To further mitigate the risk of exposing plaintext data
 969 during offloading, cryptographic techniques such as secret sharing are integrated, allowing the CPU
 970 TEE to securely partition computations, outsource them to the accelerator, and verify the correct-
 971 ness of results upon return. However, this approach remains limited in its ability to support attention
 mechanisms in Transformer-based models, which are critical to modern deep learning workloads.

972 Therefore, it is imperative to design advanced secure outsourcing schemes that preserve the CPU
 973 TEE as the single root of trust while efficiently leveraging heterogeneous and vendor-diverse un-
 974 trusted accelerators to fully exploit their performance potential without compromising security.
 975

976 F.3 SECRET SHARING FOR DATA CONFIDENTIALITY

977 Secret Sharing Cramer et al. (2015); Demmler et al. (2015) is a cryptographic primitive that allows
 978 multiple parties to compute a function over their inputs while keeping them private. All our algo-
 979 rithms are built on a two-party secret sharing over the field \mathbb{F}_p , where p is a prime number indicating
 980 field size. In a two-party secret sharing, a secret x is split into two shares by random sampling
 981 $\langle x \rangle_0, \langle x \rangle_1 \in \mathbb{F}_p$, such that $x = \langle x \rangle_0 + \langle x \rangle_1 \bmod \mathbb{F}_p$. Secret sharing offers a strong security guar-
 982 antee that, given a share $\langle x \rangle_0$ or $\langle x \rangle_1$, the value of the original x is hidden, i.e., either party can
 983 reconstruct the value of x with negligible possibility Cramer et al. (2015). In the setting of TEE-
 984 based confidential inference, the value x can be split by a randomness $r \in \mathbb{F}_p$ chosen by the TEEs,
 985 such that the two shares are $\langle x \rangle_0 = r$ and $\langle x \rangle_1 = x - r$, respectively. Prior works Tramer & Boneh
 986 (2018); Sun et al. (2023) employ secret sharing to provide privacy guarantees when outsourcing
 987 additive linear operations with constant weights w . Yet, existing outsourcing schemes cannot be
 988 extended to multiplicative attention operations where both operands are variables, such as Q and K ,
 989 as it is impossible to precompute multiplication between r and either Q or K . Even for additive
 990 linear operations, they only protect the input data x , leaving the weight matrix W exposed to the
 991 untrusted accelerator.

992 F.4 COMPUTATION VERIFICATION FOR INTEGRITY

993 The verification algorithm enables a client to assert the correctness of computations performed by
 994 a server. Within the landscape of TEEs, where computations are outsourced to high-performance
 995 untrusted devices such as GPU, ensuring the integrity of these operations is paramount. Soter (Shen
 996 et al., 2022) introduces a "fingerprint" matrix method for integrity checks by the TEEs, which, how-
 997 ever, may be vulnerable to targeted attacks. Additionally, recent research Wei et al. (2023) suggests
 998 a sampling-based verification by the TEEs to compare against GPU outputs, facing limitations in de-
 999 tecting selective manipulations without extensive sampling. Freivalds' algorithm Freivalds (1977),
 1000 referenced in Tramer & Boneh (2018); Sun et al. (2023); Hashemi et al. (2021), provides an efficient
 1001 mechanism for verifying matrix multiplications of the form $AB = C$. The algorithm commences
 1002 by generating a random vector r , followed by the TEEs computing the products $B \cdot r$ and $C \cdot r$. The
 1003 next step involves multiplying A with $B \cdot r$, and comparing this outcome to $C \cdot r$. A discrepancy
 1004 between these products indicates a failure of AB to equal C , whereas a match suggests a probable
 1005 equality between AB and C . Employing this method, the TEEs are able to perform a verification of
 1006 $\mathcal{O}(n^3)$ matrix multiplication complexity using a more efficient $\mathcal{O}(n^2)$ vector-matrix multiplication
 1007 operation, thereby enhancing the verification efficiency within the TEEs.